Int. J. Heat Mass Transfer. Vol. 34, No. 10, pp. 2497–2507, 1991
Printed in Great Britain

0017-9310/91 \$3.00+0.00
Pergamon Press plc

Conjugate heat transfer of conduction and forced convection along wedges and a rotating cone

WEN-SHING YU, HSIAO-TSUNG LIN† and TSUNG-YUAN HWANG

Department of Chemical Engineering, National Central University, Chungli, Taiwan 32054, Republic of China

(*Received* 8 *September* 1989 *and in final form* 29 *October* 1990)

Abstract—A very effective solution method is proposed to solve the conjugate problems of forced convection in laminar boundary layer flow and heat conduction in a solid wall. For flows passing a flat plate and a wedge, very accurate finite-difference solutions of interface temperature and heat transfer rates are presented over the entire thermo-fluid-dynamic field for any Prandtl number between 0.0001 and infinity. Comprehensive correlation equations of the local Nusselt numbers are also presented, which coincide excellently with the numerical data. For the conjugate problems of the stagnation flow and a rotating cone or disk, exact solutions are obtained.

1. INTRODUCTION

IN THE ordinary (traditional) convective heat transfer between a solid wall and a fluid flow, the temperature or the heat flux at the solid–fluid interface is prescribed usually as a constant over the entire interface. Physically, the condition of constant wall temperature is obtainable by mixing violently or having phase change (e.g. boiling or condensation) on the other side of a thin wall with higher thermal conductivity. In many engineering systems, however, the wall conduction resistance is not negligible. In this case, the conduction in the solid wall and convection in the fluid should be solved simultaneously. This type of conjugate heat transfer problem was introduced originally by Luikov [1]. Luikov and his co-workers solved the conjugate forced convective problem along a flat plate both numerically [2] and analytically [3–5].

In this work, we solve the same problem, but extend it to the whole ranges of the conjugation parameter and Prandtl number, by using a quite different solution method. Moreover, the conjugate problems of wedges, stagnation flow, and rotating cone or disk are also solved by the proposed method. To the knowledge of the authors, these conjugate problems have not been reported.

In the analysis of the conjugate problem, the energy conservation equations of conduction and convection are coupled by the condition of heat flux continuity at the solid–fluid interface [5]

$$-k_s\left(\frac{\partial T_s}{\partial y}\right)_{y=0} = -k_f\left(\frac{\partial T_f}{\partial y}\right)_{y=0} \tag{1}$$

where the subscripts s and f of the thermal conductivity k and temperature T are referred to the solid wall and fluid flow, respectively. In general, the axial conduction along the wall is negligible when compared with the normal conduction across the wall [4, 5]. In this case, the temperature profile in the wall is linear and equation (1) can be written as

$$k_s(T_b - T_0)/b = -k_f\left(\frac{\partial T_f}{\partial y}\right)_{y=0} \tag{2}$$

or as

$$T_b - T_0 = -\left(\frac{k_f}{k_s}b\right)\left(\frac{\partial T_f}{\partial y}\right)_{y=0} \tag{3}$$

where T_0 is the temperature at the interface of a flowing fluid and a solid wall of thickness b; and T_b the temperature at the other surface of the wall. While T_b is a specified constant, T_0 varies along the interface and depends on the flow dynamics and solid conduction in the wall.

A scale analysis on equation (3) gives

$$\frac{T_b - T_0}{T_0 - T_\infty} \sim \frac{k_f b}{k_s \delta(x)} \equiv \zeta \tag{4}$$

where $\delta(x)$ is the thickness of the thermal boundary layer. This equation defines a conjugation parameter ζ as the ratio of the thermal resistance of the solid wall to that of thermal boundary layer in fluid. The thickness of the thermal boundary layer depends on the physical properties and flow dynamics of the system. For wedges (including flat plate and two-dimensional stagnation point) in fluids of any Prandtl number, a scale analysis [6] revealed that

$$\delta(x) \sim x/Nu \sim x/[\sigma(Pr)\,Re^{1/2}] \tag{5}$$

where

$$\sigma(Pr) = Pr^{1/2}/(1+Pr)^{1/6} \tag{6}$$

and $Re = u_\infty x/\upsilon$ is the local Reynolds number. Conse-

† Author to whom correspondence should be addressed.

NOMENCLATURE

b	thickness of wall
Br_x	local Brun number
C_f	local friction coefficient
f	reduced stream function
h	local heat transfer coefficient
H	dimensionless velocity normal to the surface of a cone
I	$\int_0^\infty \exp[-\int_0^\eta f(\eta)\,d\eta]\,d\eta$
k	thermal conductivity
Nu	local Nusselt number
Pr	Prandtl number
q	heat flux
q_h	$k_s(T_b-T_\infty)/b$
q_t	$h_t(T_b-T_\infty)$
Re	local Reynolds number: $u_\infty x/\upsilon$ for wedges; and $(\omega x^2/\upsilon)\sin\phi$ for a rotating cone
T	temperature
T_b	temperature at the inner surface of the wall
T^*	dimensionless temperature, $(T-T_\infty)/(T_b-T_\infty)$
u	velocity component in the x-direction
v	velocity component in the y-direction
x	coordinate parallel to the wall
y	coordinate normal to the wall.

Greek symbols

α	thermal diffusivity of fluid
β	angle factor of the wedge
δ	thermal boundary-layer thickness
ζ	conjugation parameter, $(k_f b/k_s x)\lambda$
η	dimensionless coordinate, $(y/x)\lambda$
θ	dimensionless temperature, $(T-T_\infty)/(T_b-T_\infty)+(T-T_\infty)\lambda/(q_h x/k_f)$
λ	$\sigma\,Re^{1/2}$
υ	kinematic viscosity
ξ	dimensionless x-coordinate, $(1+\zeta)^{-1}$
ρ	fluid density
σ	$Pr^{1/2}/(1+Pr)^{1/6}$ for wedges; $Pr/(1+Pr)^{2/3}$ for rotating cone
ϕ	half angle of a cone
ψ	stream function
ω	angular velocity.

Subscripts

f	fluid
h	case of constant wall heat flux
s	solid wall
t	case of constant wall temperature
0	at the solid–fluid interface
∞	beyond the boundary layer.

quently, the conjugation parameter for a flat plate and wedges in fluids of any Prandtl number is

$$\zeta = \frac{k_f b}{k_s x}\sigma\,Re^{1/2} \tag{7}$$

which is similar to the local Brun number

$$Br_x = \frac{k_f b}{k_s x} Pr^m\,Re^n \tag{8}$$

in ref. [5]. For the conjugate problem of a flat plate in an air flow, $Br_x = (k_f b/k_s x)Pr^{1/3}\,Re^{1/2}$ [5].

For the extreme case of $\zeta \to 0$ (the wall resistance b/k_s is much less than the fluid resistance δ/k_f), it follows from equation (4) that

$$T_0 \cong T_b = \text{constant}. \tag{9}$$

This case is equivalent to the ordinary convective problem with the boundary condition of constant wall temperature. On the other hand, for the limiting case of $\zeta \to \infty$ (the wall resistance is much greater than the fluid resistance), we have

$$(T_0 - T_\infty) \ll (T_b - T_0). \tag{10}$$

This equation indicates that for the case of $\zeta \to \infty$ the temperature drop across the boundary layer is negligible when compared with that across the wall. Therefore

$$(T_b - T_0) \cong (T_b - T_\infty). \tag{11}$$

In this case, the boundary condition (2) is reduced to the ordinary boundary condition of constant wall heat flux

$$-k_f\left(\frac{\partial T_f}{\partial y}\right)_{y=0} = k_s(T_b - T_\infty)/b = \text{constant}. \tag{12}$$

The foregoing analysis reveals that the conjugate problem can be regarded as a hybrid system of the ordinary convective problem with the boundary condition of constant wall temperature and that of constant heat flux. Based on the physical nature of the conjugate problem, we propose appropriate dimensionless coordinates and temperature to give a non-similarity transformation of the energy equation over the entire thermo-fluid-dynamic field for fluids of any Prandtl number. For the extreme cases of $\zeta \to 0$ and $\zeta \to \infty$, the resulting non-similar equations can readily be reduced to the sets of similar equations of the ordinary convective problems with constant wall heat flux and constant wall temperature as boundary conditions.

For the two-dimensional stagnation flow (wedge angle $= \pi$), the non-similar energy equation is reduced to a similar equation which permits exact solution. The same form of the exact solution can be obtained for the case of a rotating cone or disk, since the transformed energy equations and boundary conditions of these two systems are very similar.

For flat plate and wedges, the non-similar equations are solved by an implicit finite-difference scheme to give very accurate results for $0 \leqslant \zeta \leqslant \infty$ and $0.0001 \leqslant Pr \leqslant \infty$. The accuracy of the numerical results is verified by comparing with the exact solution of the stagnation flow and with the previous reports for a flat plate [4, 5].

2. MATHEMATICAL FORMULATION

A schematic description of the conjugate heat transfer problems considered in this paper is shown in Figs. 1(a)–(d), respectively, for the cases of a wedge, a flat plate, the stagnation flow, and a rotating cone. Heat is transferred from the inner surface, which is kept at a constant temperature T_b, across the wall by conduction to the incompressible laminar flow of temperature T_∞ and constant properties. For convenience, the fluid temperature T_f is written as T thereafter. When the heat dissipation and body force are neglected, the boundary-layer energy equation for laminar flow over a wedge of angle $\pi\beta$ is well known as

$$u\frac{\partial T}{\partial x}+v\frac{\partial T}{\partial y}=\alpha\frac{\partial^2 T}{\partial y^2}. \tag{13}$$

The energy equation is subjected to the boundary conditions of equation (2) at the solid–fluid interface and

$$T = T_\infty \quad \text{as } y \to \infty. \tag{14}$$

For the analysis of the coupling of conduction with forced convection, we introduce the following dimensionless coordinates:

$$\eta(x,y) = y/\delta(x) = (y/x)\lambda \tag{15}$$

and

$$\xi(x) = \left(1+\frac{k_f b}{k_s x}\lambda\right)^{-1} = (1+\zeta)^{-1} \tag{16}$$

where

$$\lambda = \sigma\, Re^{1/2}. \tag{17}$$

In addition, we propose a novel dimensionless temperature

$$\begin{aligned}\theta(\xi,\eta) &= \frac{T-T_\infty}{T_b-T_\infty}+\frac{T-T_\infty}{q_h x/k_f}\lambda \\ &= \frac{T-T_\infty}{T_b-T_\infty}\left[1+\frac{k_f b}{k_s x}\lambda\right] \\ &= \frac{T-T_\infty}{T_b-T_\infty}\xi^{-1}\end{aligned} \tag{18}$$

and a reduced stream function

$$f(\eta) = \psi(x,y)/\alpha\lambda \tag{19}$$

where the constant heat flux $q_h = k_s(T_b-T_\infty)/b$. The

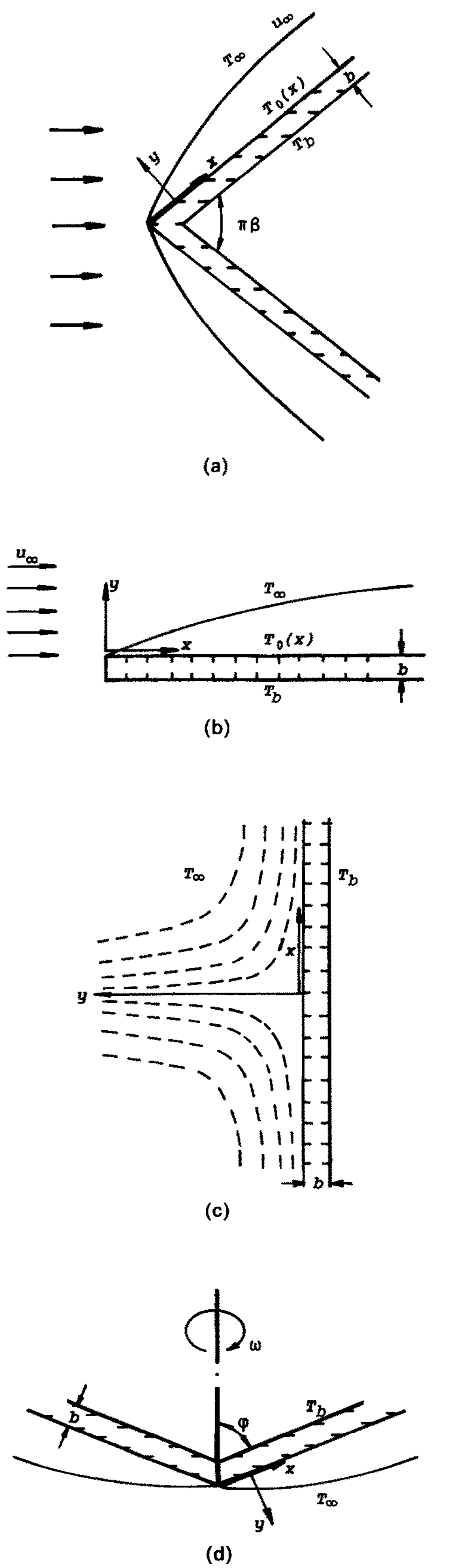

FIG. 1. Schematic diagram and coordinate system of the conjugate problems: (a) wedge; (b) flat plate; (c) stagnation point; (d) rotating cone.

energy equation (13) along with the boundary conditions (2) and (14) are then transformed into

$$\theta''+\frac{1}{2-\beta}f\theta'-\frac{1-\beta}{2-\beta}(1-\xi)f'\theta = \frac{1-\beta}{2-\beta}\xi(1-\xi)f'\frac{\partial\theta}{\partial\xi} \quad (20)$$

$$\xi\theta(\xi,0)-(1-\xi)\theta'(\xi,0) = 1 \quad (21)$$

$$\theta(\xi,\infty) = 0. \quad (22)$$

The physical quantity of most interest is the local interface temperature $\theta(\xi,0)$ from which we can determine the temperature gradient at the interface, $\theta'(\xi,0)$, by equation (21) and the local Nusselt number, $Nu = hx/k_f$, by

$$Nu/\lambda = -\theta'(\xi,0)/\theta(\xi,0) \quad (23)$$

or by

$$Nu/\lambda = \frac{1-\xi\theta(\xi,0)}{(1-\xi)\theta(\xi,0)}. \quad (24)$$

The local heat transfer rate can then be calculated by

$$q = k_s(T_b-T_0)/b = (k_s/b)(T_b-T_\infty)[1-\xi\theta(\xi,0)] \quad (25)$$

or by

$$q = h(T_0-T_\infty) = Nu\frac{k_f}{x}(T_b-T_\infty)\cdot\xi\theta(\xi,0). \quad (26)$$

The dimensionless streamwise coordinate $\xi(x)$ is also an alternative form of the conjugation parameter ζ or the local Brun number in ref. [5]. For the limiting case of $\xi = 0$ ($\zeta\to\infty$), equations (20), (21) and (23) are reduced, respectively, to

$$\theta''+\frac{1}{2-\beta}f\theta'-\frac{1-\beta}{2-\beta}f'\theta = 0 \quad (27)$$

$$\theta'(0,0) = -1 \quad (28)$$

and

$$Nu_h/\lambda = 1/\theta(0,0). \quad (29)$$

While for the other limiting case of $\xi = 1$ ($\zeta = 0$), the reduced equations are

$$\theta''+\frac{1}{2-\beta}f\theta' = 0 \quad (30)$$

$$\theta(1,0) = 1 \quad (31)$$

and

$$Nu_t/\lambda = -\theta'(1,0). \quad (32)$$

The former and the latter sets of similar equations are identical to those of the ordinary convective problems [6] with the boundary conditions of constant wall heat flux and constant wall temperature, respectively.

3. NUMERICAL SOLUTION

Equations (20)–(22) are solved by a very effective finite-difference scheme known as Keller's box method [7]. The numerical integration was carried out step-by-step from $\xi = 0$ to 1 with uniform step size $\Delta\xi = 0.01$. To obtain numerical results of high accuracy, the step size $\Delta\eta$ was taken to be 0.05 and the integration was ended at $\eta_\infty = 6$.

In the numerical integration of equation (20), the values of $f(\eta)$ and $f'(\eta)$ at each η were obtained from the numerical integration of the transformed momentum equation [6]

$$Pr\,f'''+\frac{1}{2-\beta}ff''+\frac{\beta}{2-\beta}[(1+Pr)^{2/3}-f'f'] = 0 \quad (33)$$

with the boundary conditions

$$f(0) = 0,\quad f'(0) = 0,\quad f''(0) = 0.5(1+Pr^{-1})^{1/2}C_f\,Re^{1/2} \quad (34)$$

by using a fourth-order Runge–Kutta scheme. The values of $C_f\,Re^{1/2}$ are 0.66412, 1.51490, and 2.465175 [6] for the cases of a flat plate ($\beta = 0$), a wedge of $\beta = 0.5$, and the stagnation flow ($\beta = 1$), respectively.

4. EXACT SOLUTIONS FOR STAGNATION FLOW AND ROTATING CONE

For the stagnation flow ($\beta = 1$), equation (20) is reduced to the similar equation

$$\theta''+f\theta' = 0. \quad (35)$$

Via separation of variables, equation (35) can be integrated to yield

$$\theta'(\xi,\eta) = \theta'(\xi,0)\exp\left[-\int_0^\eta f(\eta)\,d\eta\right]. \quad (36)$$

Integrating equation (36) from η to ∞ and using the boundary condition (22), we obtain

$$\theta(\xi,\eta) = -\theta'(\xi,0)\int_\eta^\infty \exp\left[-\int_0^\eta f(\eta)\,d\eta\right]d\eta. \quad (37)$$

At the solid–fluid interface

$$\theta(\xi,0) = -\theta'(\xi,0)\int_0^\infty \exp\left[-\int_0^\eta f(\eta)\,d\eta\right]d\eta. \quad (38)$$

The integral of the exponential function in equation (38) can be regarded as a known constant for a given Prandtl number. Thus equation (38) can be rewritten as

$$\theta(\xi,0) = -\theta'(\xi,0)I(Pr). \quad (39)$$

From equations (23) and (39), we find

$$Nu/\lambda = -\theta'(\xi,0)/\theta(\xi,0) = 1/I(Pr). \quad (40)$$

This equation reveals that, for a specified Pr, Nu/λ is a constant for any conjugation parameter ξ. Consequently, the values of $I(Pr)$ can be obtained from the numerical results of $\theta(0,0)$ at $\xi = 0$ and $\theta'(1,0)$ at $\xi = 1$. At $\xi = 0$, $\theta'(0,0) = -1$ and thus

$$I(Pr) = \theta(0,0). \quad (41)$$

On the other hand, at $\xi = 1$, $\theta(1,0) = 1$ and therefore

$$I(Pr) = -1/\theta'(1,0). \quad (42)$$

The values of $\theta(0,0)$ and $\theta'(1,0)$ for $Pr = 0.0001$ to infinity can be found from Tables 1 and 2 of ref. [6]. From equations (21) and (39), we obtain the exact solutions of the interface temperature

$$\theta(\xi,0) = I/[1-(1-I)\xi] \quad (43)$$

and the temperature gradient at the interface

$$\theta'(\xi,0) = -1/[1-(1-I)\xi]. \quad (44)$$

For the conjugate problem of a rotating cone or disk, the transformed energy equation is derived as

$$\theta'' - H\theta' = 0 \quad (45)$$

where the dimensionless velocity $H = vx/\alpha\lambda$. The variable λ in the definitions of H, ζ, η, ξ, and θ is defined as

$$\lambda = \sigma Re^{1/2} = [Pr/(1+Pr)^{2/3}][(\omega x^2/\nu)\sin\phi]^{1/2} \quad (46)$$

where ω is the angular velocity and ϕ the half angle of the rotating cone. For the special case of $\phi = \pi/2$, the rotating cone is reduced to a rotating disk.

Since the transformed energy equations (35) and (45) are very similar and are subjected to the same boundary conditions, the exact solutions of $\theta(\xi,\eta)$, $\theta(\xi,0)$, $\theta'(\xi,0)$, and Nu/λ derived for the case of the stagnation flow can be applied to that of a rotating cone, except that $f(\eta)$ in equations (37) and (38) is replaced by $-H(\eta)$. The values of $\theta(0,0)$ and $\theta'(1,0)$ for a rotating cone were listed in Table 1 of ref. [8] for $Pr = 0.001$ to infinity. These values can also be obtained from a correlation equation in ref. [8] or from the more precise correlation

$$Nu_h/\lambda = 1/\theta(0,0) = Nu_t/\lambda = -\theta'(1,0)$$
$$= 0.6109\left[\frac{1+Pr}{0.5301+0.3996Pr^{1/2}+Pr}\right]^{2/3}. \quad (47)$$

The maximum error of this correlation is less than 4% for any Prandtl number between 0.001 and infinity.

5. RESULTS AND DISCUSSIONS

5.1. *Temperature profiles*

Typical dimensionless temperature profiles $\theta(\xi,\eta)$ for the case of a flat plate are presented in Figs. 2 and 3, respectively, for fluids of very small ($Pr = 0.001$) and moderate ($Pr = 0.7$) Prandtl numbers. The temperature profiles for large Prandtl numbers ($Pr \geqslant 7$) are very similar to those for $Pr = 0.7$. The temperature profiles of wedges are similar to those of a flat plate, and are left out here. The profiles of a different dimensionless temperature

$$T^* = \frac{T-T_\infty}{T_b-T_\infty} = \xi\theta(\xi,\eta) \quad (48)$$

are shown in Fig. 4 for a flat plate ($\beta = 0$) in air ($Pr = 0.7$). As can be seen in this figure, the interface temperature increases from T_∞ at $\xi = 0$ to T_b at $\xi = 1$. Figures 3 and 4 show clearly the evolution of the temperature profiles from the profile of the constant

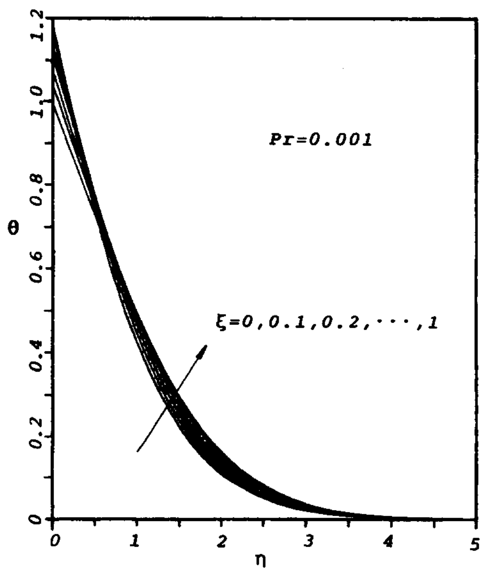

FIG. 2. Typical dimensionless temperature profiles $\theta(\xi,\eta)$ for a flat plate, $Pr = 0.001$.

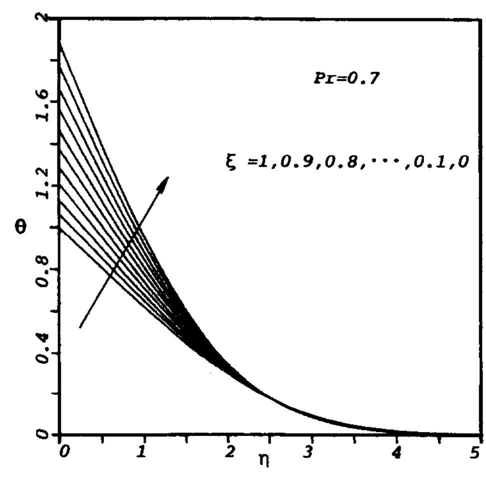

FIG. 3. Typical dimensionless temperature profiles $\theta(\xi,\eta)$ for a flat plate, $Pr = 0.7$.

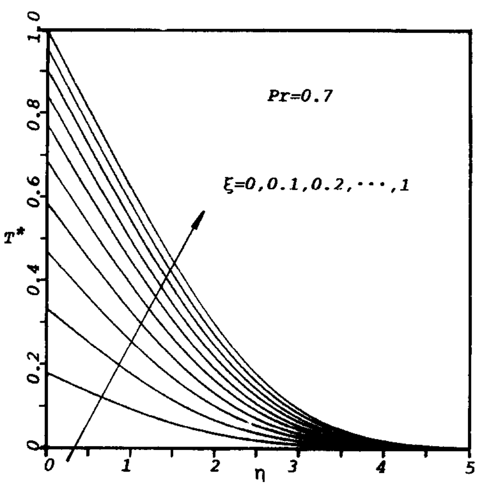

FIG. 4. Typical dimensionless temperature profiles T^* for a flat plate in an air flow ($Pr = 0.7$).

wall heat flux case ($\xi = 0$) to that of the constant wall temperature case ($\xi = 1$).

5.2. *Interface temperature*

Numerical results of the interface temperature $\theta(\xi, 0)$ for the conjugate problems of a flat plate ($\beta = 0$) and a wedge of $\beta = 0.5$ are listed respectively in Tables 1 and 2 for $Pr = 0.0001$ to infinity. For the cases of the stagnation flow and a rotating cone, exact solution (43) is available, and the numerical data of these cases are not presented here to conserve space. The accuracy of the numerical results is confirmed by comparing with the exact solutions of the stagnation flow. It is found that the two solutions are identical even to the fifth significant digit. In addition, at $\xi = 0$ the present results of $\theta(0,0)$ are identical to the previous results [6] of the ordinary convective problems with constant wall heat flux. Furthermore, at $\xi = 1$, all the numerical results of $\theta'(1,0)$ are identical to those for the constant wall temperature case [6].

The variations of the dimensionless interface temperature

$$T_0^* = \frac{T_0 - T_\infty}{T_b - T_\infty} = \xi\theta(\xi, 0) \tag{49}$$

with $1/\zeta$ are shown in Fig. 5 for the case of a flat plate. For the cases of a wedge of $\beta = 0.5$ and the stagnation flow ($\beta = 1$) as well as rotating cone or disk, the plots of the dimensionless interface temperature are similar to this figure and are omitted here. Figure 5 shows that the interface temperature increases as Prandtl number increases from 0.0001 to 10 for large conjugation parameter. However, the interface temperature is almost independent of Prandtl number for $Pr \geqslant 10$. This figure also shows that, for any Prandtl number, the dimensionless interface temperature

Table 1. Numerical results of $\theta(\xi, 0)$ for the case of a flat plate

	Pr											
ζ	0.0001	0.001	0.01	0.1	0.7	1	7	10	100	1000	10 000	∞
0.0	1.14560	1.18147	1.28721	1.55113	1.88680	1.94106	2.11244	2.12496	2.15331	2.15632	2.15662	2.15665
0.1	1.15526	1.18711	1.27987	1.50432	1.77632	1.81895	1.95118	1.96071	1.98220	1.98447	1.98470	1.98472
0.2	1.16161	1.18916	1.26841	1.45443	1.66958	1.70232	1.80222	1.80932	1.82529	1.82698	1.82714	1.82716
0.3	1.16378	1.18683	1.25234	1.40172	1.56717	1.59167	1.66535	1.67053	1.68214	1.68336	1.68348	1.68350
0.4	1.16080	1.17928	1.23121	1.34659	1.46959	1.48738	1.54022	1.54389	1.55211	1.55298	1.55306	1.55307
0.5	1.15168	1.16568	1.20469	1.28954	1.37725	1.38970	1.42630	1.42882	1.43446	1.43505	1.43511	1.43512
0.6	1.13552	1.14537	1.17266	1.23122	1.29046	1.29875	1.32296	1.36462	1.32832	1.32871	1.32875	1.32876
0.7	1.11174	1.11801	1.13534	1.17234	1.20938	1.21452	1.22947	1.23050	1.23277	1.23301	1.23303	1.23304
0.8	1.08042	1.08385	1.09335	1.11368	1.13403	1.13686	1.14504	1.14560	1.14685	1.14698	1.14699	1.14700
0.9	1.04255	1.04393	1.04776	1.05601	1.06433	1.06548	1.06884	1.06907	1.06958	1.06963	1.06964	1.06965
1.0	1.00000	1.00000	1.00000	1.00000	1.00000	1.00000	1.00000	1.00000	1.00000	1.00000	1.00000	1.00000

Table 2. Numerical results of $\theta(\xi, 0)$ for the case of a wedge with $\beta = 0.5$

	Pr											
ζ	0.0001	0.001	0.01	0.1	0.7	1	7	10	100	1000	10 000	∞
0.0	1.18077	1.20134	1.26264	1.41812	1.61401	1.64378	1.71960	1.72146	1.70999	1.69733	1.69082	1.68514
0.1	1.18076	1.19886	1.25236	1.38546	1.54798	1.57214	1.63267	1.63404	1.62422	1.61373	1.60835	1.60365
0.2	1.17741	1.19295	1.23854	1.34984	1.48165	1.50085	1.54813	1.54909	1.54083	1.53231	1.52795	1.52413
0.3	1.17023	1.18320	1.22094	1.31142	1.41554	1.43041	1.46642	1.46707	1.46029	1.45351	1.45004	1.44702
0.4	1.15880	1.16923	1.19937	1.27045	1.35015	1.36132	1.38797	1.38839	1.38297	1.37771	1.37503	1.37269
0.5	1.14277	1.15079	1.17381	1.22733	1.28602	1.29412	1.31315	1.31339	1.30921	1.30527	1.30327	1.30152
0.6	1.12200	1.12782	1.14441	1.18256	1.22366	1.22926	1.24222	1.24235	1.23928	1.23646	1.23503	1.23378
0.7	1.09665	1.10053	1.11157	1.13675	1.16353	1.16714	1.17539	1.17545	1.17335	1.17146	1.17050	1.16967
0.8	1.06723	1.06951	1.07595	1.09059	1.10602	1.10809	1.11275	1.11277	1.11150	1.11038	1.10982	1.10932
0.9	1.03464	1.03563	1.03843	1.04479	1.05145	1.05233	1.05431	1.05432	1.05374	1.05325	1.05300	1.05278
1.0	1.00000	1.00000	1.00000	1.00000	1.00000	1.00000	1.00000	1.00000	1.00000	1.00000	1.00000	1.00000

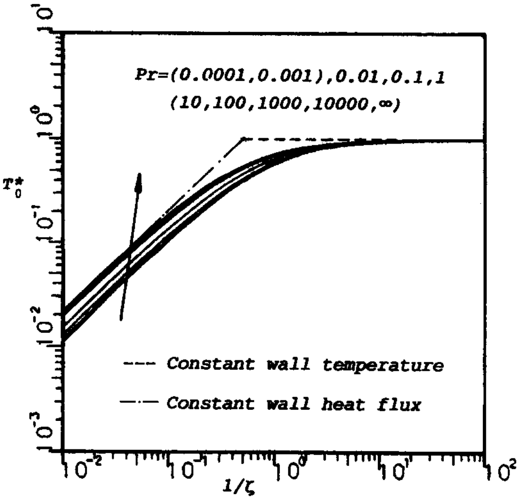

FIG. 5. Variations of the dimensionless interface temperature T_0^* with $1/\zeta$ for a flat plate.

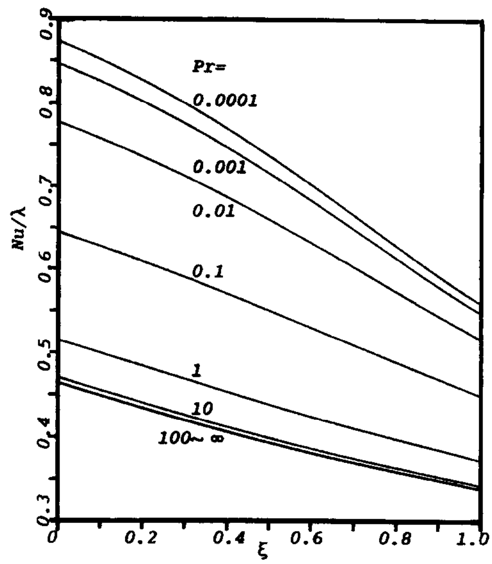

FIG. 7. Variations of Nu/λ with ξ for a flat plate.

increases with decreasing ζ or with increasing x, since $1/\zeta$ is proportional to $x^{1/2}$ for a specified solid wall and fluid flow.

The effect of wedge angle on the interface temperature is shown in Fig. 6 for $Pr = 0.7$. This figure shows that T_0 decreases as β increases at any ξ except $\xi = 0$ and 1. At the leading edge ($x = 0$, $\xi = 0$) $T_0 = T_\infty$, while at a downstream distance far from the leading edge ($x/b \to \infty$, $\xi = 1$) $T_0 = T_b$, for any configuration of wedge.

5.3. *Local Nusselt number*

From the numerical results of $\theta(\xi, 0)$, the local Nusselt number can be calculated by using equation (24). The variations of the local Nusselt number with the conjugation parameter can be seen from a plot of Nu/λ vs ξ, or from an equivalent plot of $N^* = Nu/Nu_t$ vs $1/\zeta$, where Nu_t is the local Nusselt number of the ordinary convective problem with the boundary condition of constant interface temperature. The first kind of plot is presented in Fig. 7 for a flat plate ($\beta = 0$). While the second kind of plot is presented in Figs. 8 and 9. It is seen from Fig. 7 that Nu/λ decreases almost linearly with increasing ξ for any Prandtl number. This linear relationship has the benefit of the proper definition of ξ. Figure 8 shows that, for any Pr, the local Nusselt number of a flat plate decreases from one asymptote to the other as ζ decreases (ξ increases). This figure also reveals that the local Nusselt number decreases with increasing the downstream distance x, since $1/\zeta$ is proportional to $x^{1/2}$.

Figure 9 shows that N^* decreases as ζ decreases for both the cases of a flat plate and a wedge of $\beta = 0.5$.

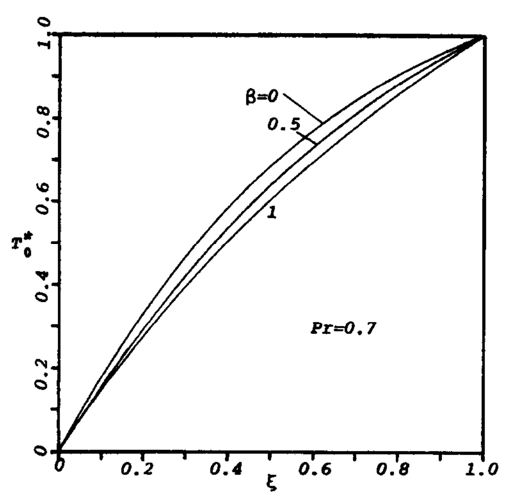

FIG. 6. Effect of wedge angle on the dimensionless interface temperature T_0^*, $Pr = 0.7$.

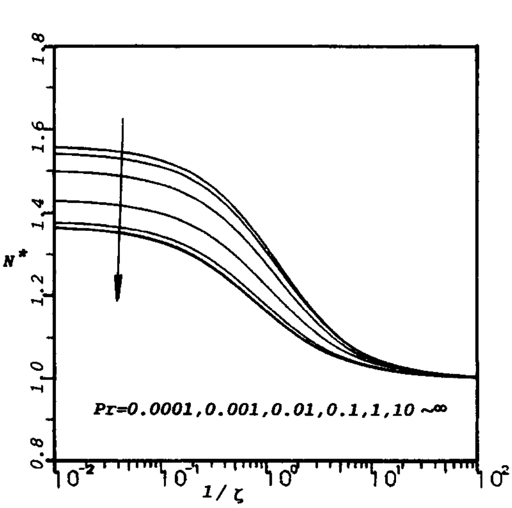

FIG. 8. Variations of N^* with $1/\zeta$ for a flat plate.

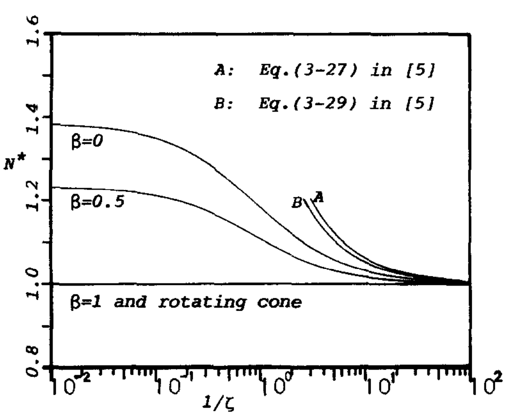

FIG. 9. Comparisons of N^*

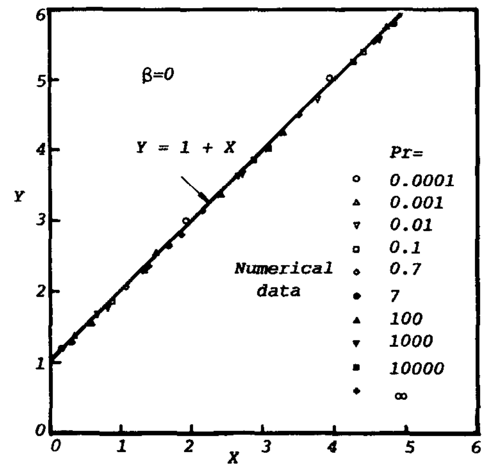

FIG. 10. A comparison between the correlated and calculated local Nusselt numbers of a flat plate.

However, for the cases of the stagnation flow and a rotating cone, the local Nusselt number is a constant for any ζ or ξ, as can be seen from this figure and has been indicated in equation (40). Formulas (3.27) and (3.29) of ref. [5] for a flat plate in air and for small Brun numbers are also plotted in Fig. 9 for comparison. The comparison reveals good agreement between these formulas and the present numerical solution for small values of ζ. The local Brun number in these formulas has been converted to ζ by multiplying by a factor of $(1+Pr^{-1})^{1/6}$.

5.4. *Correlations of the local Nusselt number*

The linear relationship between Nu/λ and ξ shown in Fig. 7 leads to a simple but very accurate correlation. We propose here a correlation equation of the local Nusselt number for the conjugate problem as

$$Nu = (1-\xi)Nu_h + \xi\, Nu_t \tag{50}$$

where Nu_h and Nu_t are the local Nusselt numbers of ordinary convective problems with constant wall heat flux and constant wall temperature, respectively. For a flat plate, we have introduced, in ref. [9], the following correlations of very high accuracy (maximum error < 1.4%) for $0.0001 \leqslant Pr \leqslant \infty$:

$$Nu_h/\lambda = 0.4689\left[\frac{1+Pr}{0.0247+0.0987Pr^{1/2}+Pr}\right]^{1/6} \tag{51}$$

$$Nu_t/\lambda = 0.3386\left[\frac{1+Pr}{0.0526+0.1121Pr^{1/2}+Pr}\right]^{1/6}. \tag{52}$$

For a wedge of $\beta = 0.5$, we propose here the following correlation equations:

$$Nu_h/\lambda = 0.5934\left[\frac{1+Pr}{0.1182+0.6036Pr^{1/2}+Pr}\right]^{1/6} \tag{53}$$

$$Nu_t/\lambda = 0.4908\left[\frac{1+Pr}{0.1828+0.7415Pr^{1/2}+Pr}\right]^{1/6} \tag{54}$$

for $0.0001 \leqslant Pr \leqslant \infty$. The maximum discrepancy between the predicted values from the correlation equations and the numerical results is less than 0.9% over the entire region of $0.0001 \leqslant Pr \leqslant \infty$.

Equation (50) can be rewritten as

$$Y = 1+X \tag{55}$$

where

$$Y = \frac{Nu}{Nu_h}\frac{1}{1-\xi} \tag{56}$$

and

$$X = \frac{Nu_t}{Nu_h}\frac{\xi}{1-\xi}. \tag{57}$$

Comparisons between the correlations and the numerical data are made in Figs. 10 and 11 for a

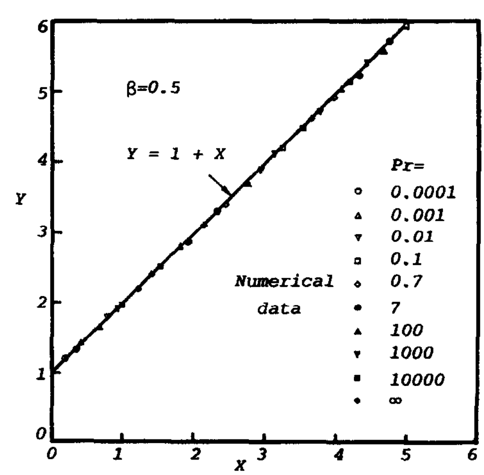

FIG. 11. A comparison between the correlated and calculated local Nusselt numbers of a wedge with $\beta = 0.5$.

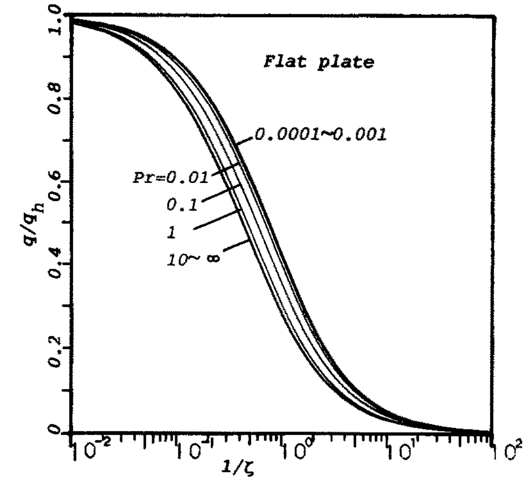

FIG. 12. Variations of the local heat transfer rates with $1/\zeta$ for a flat plate.

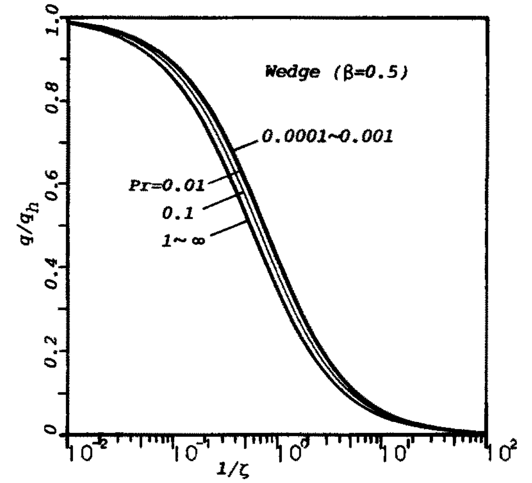

FIG. 13. Variations of the local heat transfer rates with $1/\zeta$ for a wedge of $\beta = 0.5$.

flat plate and a wedge of $\beta = 0.5$, respectively. These figures have shown excellent agreement between the proposed correlations and the numerical results. For the case of a flat plate, the maximum deviation is less than 2.8% for $0.001 \leqslant Pr \leqslant \infty$, and 4.1% for $Pr = 0.0001$. For a wedge of $\beta = 0.5$, the maximum discrepancy is less than 1.9% for $0.0001 \leqslant Pr \leqslant \infty$.

5.5. *Local heat transfer rate*

The local heat transfer rate can be calculated either by equation (25) or by equation (26). These two equations can be rewritten, respectively, as

$$q/q_h = 1-\xi\theta(\xi,0) \tag{58}$$

and

$$q/q_t = [\theta'(\xi,0)/\theta'(1,0)]\xi \tag{59}$$

where

$$q_t = h_t(T_b - T_\infty) = Nu_t(k_f/x)(T_b - T_\infty) \tag{60}$$

is the local heat transfer rate of the constant wall temperature case. For the cases of the stagnation flow and a rotating cone, the values of $\theta(\xi,0)$ in equation (58) and $\theta'(\xi,0)$ in equation (59) can be obtained from the exact solutions (43) and (44), respectively. While for the cases of a flat plate and a wedge of $\beta = 0.5$, values of $\theta(\xi,0)$ are obtainable either from Tables 1 and 2 or from the correlation equations (50)–(54) for Nu/λ together with equation (24). Once values of $\theta(\xi,0)$ are at hand, values of $\theta'(\xi,0)$ can be calculated from equation (21) except for the values of $\theta'(1,0)$ at $\xi = 1$, which can be obtained from ref. [6].

The variations of the dimensionless local heat transfer rate q/q_h with $1/\zeta$ are shown in Figs. 12–15 for wedges of $\beta = 0$, 0.5, 1 and a rotating cone, respectively. These figures show that q/q_h decreases with increasing $1/\zeta$ or x. The decrease of heat transfer rate along the downstream distance is a result of the decrease of temperature difference across the wall and the increase of the boundary layer thickness. Further inspection of these figures reveals that q approaches q_h at large values of ζ. In this region, the conjugate problem can be approximated by the ordinary convective problem with a boundary condition of constant heat flux. On the other hand, there is a region of small values of ζ where q/q_h vanishes. In this region, the local heat transfer rate should be calculated by using equation (59). A very small conjugation parameter implies that the wall is very thin and its thermal conductivity is very large. In this case, the system is equivalent to the ordinary convective problem with $T_0 = T_b$ = constant as the boundary condition.

Table 3 shows a summary of the regimes of the conjugation parameter ζ, in which a convective system should be solved as a conjugate problem. Beyond these regimes, a convective system can be approxi-

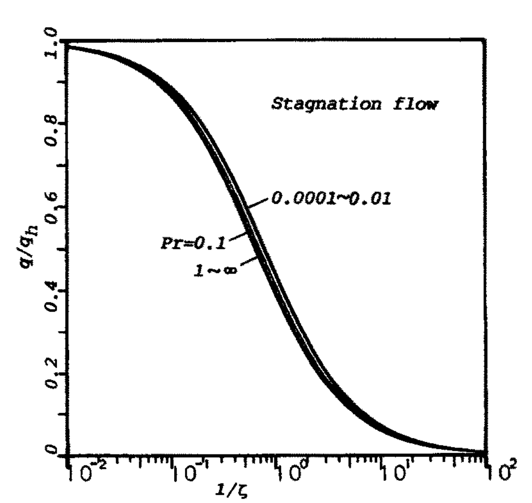

FIG. 14. Variations of the local heat transfer rates with $1/\zeta$ for the stagnation flow.

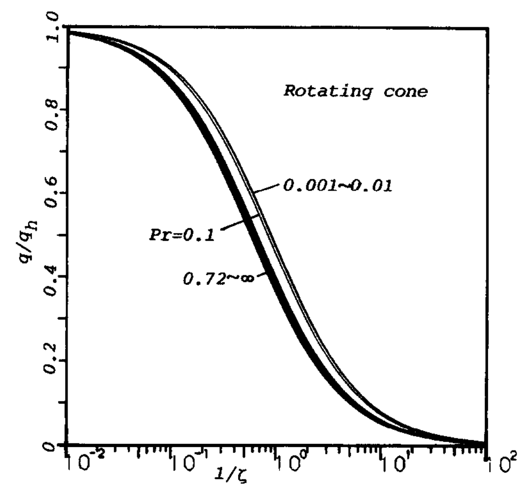

FIG. 15. Variations of the local heat transfer rates with $1/\zeta$ for a rotating cone.

mated, within 5% error of the local heat transfer rate, by the ordinary forced convection with boundary condition of constant wall heat flux or constant wall temperature.

It follows from equations (48) and (58) that

$$q/q_h = 1 - T_0^* = \frac{T_b - T_0}{T_b - T_\infty}. \tag{61}$$

Therefore, Figs. 12–15 also show the variations of the dimensionless interface temperature $(T_b - T_0)/(T_b - T_\infty)$. As can be seen from these figures, the interface temperature increases from T_∞ to T_b as $1/\zeta$ or the downstream distance increases.

6. CONCLUSIONS

In this paper, we have introduced a new solution method for the analyses of the conjugate problems of conduction in solid and forced convection in fluid flow. This method is based on the nature of the conjugate problem as a hybrid system of the ordinary convective problem with constant wall temperature and that with constant wall heat flux. All the variables are defined in such a way to reflect the characteristic of the conjugate problem. The analyses and results have shown that this method is physically strict, mathematically simple and very accurate. With some modifications, the method can be applied to the conjugate problems of free convection on vertical and horizontal flat plates [10].

The correlation equations presented for a flat plate and a wedge of $\beta = 0.5$ are valid over the entire thermo-fluid-dynamic field for $0.0001 \leqslant Pr \leqslant \infty$. These correlation equations and the exact solutions for the stagnation flow and a rotating cone are very useful and reliable for engineering applications. Moreover, we have also presented the regimes of the conjugation parameter in which a convective system should be solved as a conjugate problem. Beyond this regime, the system can be approximated, within 5% error, by the ordinary convective problem of constant wall temperature or constant wall heat flux.

Table 3. The regimes of ζ in which a convection system should be solved as a conjugate problem

Pr	Flat plate	Wedge ($\beta = 0.5$)	Stagnation	Rotating cone
0.0001	(0.33, 24)	(0.12, 24)	(0.064, 24)	—
0.001	(0.33, 24)	(0.12, 24)	(0.064, 32)	(0.053, 24)
0.01	(0.33, 32)	(0.12, 32)	(0.064, 32)	(0.053, 24)
0.1	(0.33, 32)	(0.14, 32)	(0.064, 32)	(0.064, 24)
$\geqslant 1$	(0.37, 49)	(0.15, 32)	(0.075, 32)	(0.075, 32)

Acknowledgement—This work was supported by a National Science Council Grant.

REFERENCES

1. A. V. Luikov, *Analytical Heat Diffusion Theory*. Academic Press, New York (1968).
2. A. V. Luikov, T. L. Perelman and V. B. Ryvkin, On determination of heat transfer coefficient in simultaneous conductive and convective heat transfer processes, 3rd Int. Heat Transfer Conf., Chicago (1966).
3. A. V. Luikov, V. A. Aleksashenko and A. A. Aleksashenko, Analytical methods of solution of conjugated problem in convective heat transfer, *Int. J Heat Mass Transfer* **14,** 1047–1056 (1971).
4. A. V. Luikov, *Heat and Mass Transfer*, Handbook. Energiya, Moscow (1972).
5. A. V. Luikov, Conjugate convective heat transfer problems, *Int. J. Heat Mass Transfer* **17,** 257–265 (1974).
6. H.-T. Lin and L.-K. Lin, Similarity solutions for laminar forced convection heat transfer from wedges to fluids of any Prandtl number, *Int. J. Heat Mass Transfer* **30,** 1111–1118 (1987).
7. T. Cebeci and P. Bradshaw, *Physical and Computational Aspects of Convective Heat Transfer*. Springer, New York (1984).
8. H.-T. Lin and L.-K. Lin, Heat transfer from a rotating cone or disk to fluids of any Prandtl number, *Int. Commun. Heat Mass Transfer* **14,** 323–332 (1987).
9. H.-T. Lin, W.-S. Yu and C.-C. Chen, Comprehensive correlations for laminar mixed convection on vertical and horizontal flat plates, *Warme- und Stoffübertrag.* **25,** 353–359 (1990).
10. W.-S. Yu and H.-T. Lin, Conjugate problems of conduction and free convection on vertical and horizontal flat plates, *Int. J. Heat Mass Transfer* (under review).

TRANSFERT THERMIQUE COUPLE DE CONDUCTION ET DE CONVECTION FORCEE LE LONG DES ANGLES ET D'UN CONE TOURNANT

Résumé—On propose une méthode de résolution trés efficace pour traiter les problèmes couplés de convection forcée pour les écoulements à couche limite et de conduction dans une paroi solide. Pour des écoulements sur une plaque plane et un angle, des solutions très précises aux différences finies de température à l'interface et de flux thermique sont présentées pour un nombre de Prandtl entre 0,0001 et l'infini. Des équations donnant le nombre de Nusselt local sont présentées qui coincident parfaitement avec les données numériques. Pour les problèmes couplés de l'écoulement d'arrêt et un cone ou un disque tournant, on obtient des solutions exactes.

KONJUGIERTE WÄRMEÜBERTRAGUNG DURCH LEITUNG UND ERZWUNGENE KONVEKTION UM EINEN KEIL UND EINEN ROTIERENDEN KEGEL

Zusammenfassung—Es wird ein sehr effizientes Lösungsverfahren zur Behandlung des konjugierten Problems der erzwungenen Konvektion in einer laminaren Grenzschichtströmung und der Wärmeleitung in einer festen Wand vorgeschlagen. Für Strömungen entlang einer ebenen Platte und über einen Keil werden unter Verwendung eines Finite-Differenzen-Verfahrens sehr genaue Ergebnisse für die Grenzflächentemperatur und den Wärmeübergang vorgestellt, und zwar im gesamten thermo-fluiddynamischen Bereich bei beliebiger Prandtl-Zahl zwischen 0,0001 und unendlich. Für die örtliche Nusselt-Zahl wird außerdem eine Korrelationsgleichung angegeben, mit deren Hilfe die numerischen Daten hervorragend wiedergegeben werden können. Für die konjugierten Probleme einer Staupunktströmung und eines rotierenden Zylinders oder einer rotierenden Scheibe ergeben sich exakte Lösungen.

СОПРЯЖЕННЫЙ ТЕПЛОПЕРЕНОС ПРИ ОБТЕКАНИИ КЛИНЬЕВ И ВРАЩАЮЩЕГОСЯ КОНУСА

Аннотация—Предложен эффективный метод решения сопряженной задачи теплообмена в ламинарном пограничном слое и теплопроводности в твердой стенке. В случае обтекания плоской пластины и клина представлены конечно-разностные решения для температуры и теплового потока на границе раздела при значениях числа Прандтля, изменяющихся от 0,0001 до бесконечности. Приводятся также обобщающие соотношения для локальных чисел Нуссельта, которые очень хорошо согласуются с численными результатами. Получены решения сопряженных задач течения вблизи критической точки, а также вращающегося конуса или диска.